Chapter 34
Deformation Capacity of Lightly Reinforced Concrete Members – Comparative Evaluation

S.J. Pantazopoulou and D.V. Syntzirma

34.1 Introduction

Research towards development of expressions for estimating the deformation capacity of R.C. members may be traced back to the time when strength expressions were first established [9]. However, the success in the area of deformation prediction is far more limited. For example, whereas the lateral load strength of a simple structure such as a well detailed cantilever R.C. column may be quantified with a margin of error within 10% of the actual value, the estimated drift capacity with the available tools today may be as far off as 100% of the actual value, with a generally inestimable and uncertain margin of safety.

This uncertainty is particularly relevant in displacement based assessment, where the assessment verdict explicitly rides on the ability of the member to sustain the imposed drift demand, and is reflected by the large factors of safety used to obtain design values [3, 5, 4]. A number of issues regarding behaviour of the response mechanisms in R.C. are considered responsible for the scatter. The paper reviews the mechanics of deformation of R.C. members and methods of evaluation of deformation resultants at advanced stages of inelastic response. A comparative study of consistently estimated deformation capacities with estimates obtained from Codes is conducted on a series of column-specimens tested under reversed cyclic load simulating earthquake effects; the specimens modelled former detailing practices representative of the 1950s–1970s [14, 12]. The models' performance in assessing the dependable deformation capacity is interpreted with reference to the important mechanisms controlling the observed specimen behaviour.

S.J. Pantazopoulou (✉)
Department of Civil Engineering, Demokritus University of Thrace, Vas. Sofias Str., No. 12, Xanthi, 67100, Greece
e-mail: pantaz@civil.duth.gr

M.N. Fardis (ed.), *Advances in Performance-Based Earthquake Engineering*, Geotechnical, Geological, and Earthquake Engineering 13, DOI 10.1007/978-90-481-8746-1_34,

34.2 Deformation Mechanisms in R.C. Members

Behavior of R.C. frame members under combined axial load, and cyclic shear – flexure, such as occurring during earthquakes, is usually interpreted with the model of Fig. 34.1a. The static relationship between shear force and flexural moment in the span of the cantilever (Fig. 34.1a) is identical to that occurring over the length of the actual frame member extending from the point of contraflexure (zero moment) to the fixed end support. Deformations are owing to flexure, shear action, and pullout slip of the reinforcement from the support or lap splice; these mechanisms of behaviour are considered to act in series, therefore their effects are considered additive, as implied by the mechanical analogue of Fig. 34.1b, used in computer simulations of inelastic R.C. members. Elastic curvature over the member's length contributes to total drift, whereas all other effects (inelastic rotation over the plastic hinge region, shear deformation and pullout slip) are modelled through pertinent springs, each characterized by an individual resistance curve (Fig. 34.1c).

These mechanisms were originally assumed to act independently of each other. The total deformation obtained for any given load combination was approximated by the summation of the individual contributions (Fig. 34.2). The same concept was extended to deformation *capacity* which is a measure of total deformation that the member may undergo without significant irreversible loss of strength; for frame members this is usually quantified by the chord rotation θ_u, associated with a 20% loss of strength beyond the peak point.

The idea that deformation capacity may be estimated as the sum of contributions of the participating mechanisms was tested against hundreds of tests contained in many databases, including R.C. members with modern detailing as well as members

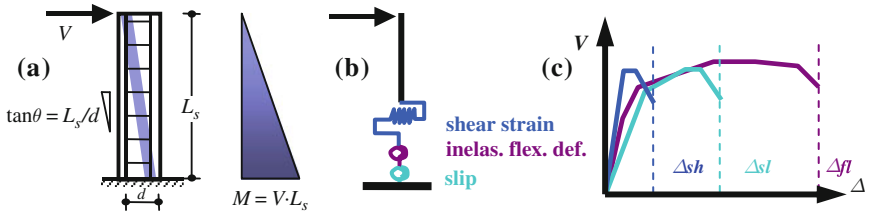

Fig. 34.1 (**a**) Idealization of shear span as a cantilever, (**b**) mechanistic analogue (**c**) resistance curves of individual springs, each having a different strength: $V_{u,\mathrm{fl}}$, $V_{u,\mathrm{sh}}$, $V_{u,\mathrm{sl}}$

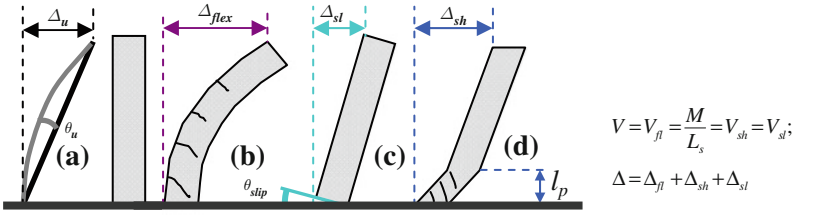

Fig. 34.2 Contribution of the various response mechanisms to the total drift

with substandard details representative of old design practices [9, 8, 13, 7, 1]. Realistic values are obtained for well detailed members, which generally demonstrate large deformation capacity particularly when their axial load ratio is less than 0.4. The values become irrelevant when this concept is applied to members experiencing brittle failure, as often encountered with old-type frame members. Clearly, if the strength of one of the springs in the assembly of Fig. 34.1b is overcome at some value of deformation, then this event terminates the response curve of the member, well before the development of the estimated nominal deformation capacity of the other springs. This is why, of late, this approach has been retained only to describe behaviour up to the onset of yielding, i.e., $\theta_y=\theta_{y,\mathrm{fl}}+\theta_{y,\mathrm{sl}}+\theta_{y,\mathrm{sh}}$. For response beyond yielding, opinions diverge as to how to estimate deformation capacity.

Thus, the revised ASCE-41 document [4], which reflects the recommended N.A. assessment practice, evaluates directly the total inelastic drift capacity, θ_u, through empirical rules, the result being a single compound value that accounts for the various effects and design parameters through pertinent binary rules: here, the total rotation capacity is, $\theta_u=\theta_y+\theta_{\mathrm{pl}}$. Similar is the approach drafted for the revised EC8-III, which provides direct estimates for the total inelastic rotation capacity, θ_u, through calibrated expressions in terms of the relevant design variables (revised draft of [3]).

Recognizing the fundamental relevance of the model depicted in Fig. 34.1b the authors attempted to improve on its correlation with the test data, by modifying the additive expression, so that contributions of the individual contributing mechanisms were associated with the onset of occurrence of any type of premature failure [15]. This framework was referred to as *Capacity – Based Prioritizing* of failure modes (CBP):

$$\Delta_y = w_y \cdot [\Delta_{y,fl} + \Delta_{y,\mathrm{sh}} + \Delta_{y,\mathrm{sl}}]\ \Delta_u = \Delta_{y,\mathrm{fl}} + w_u \cdot [\Delta_{p,\mathrm{fl}} + \Delta_{p,\mathrm{sh}} + \Delta_{p,\mathrm{sl}}] \quad (34.1)$$

Factors w_y, w_u, represent strength or deformation ratios for strength-controlled or strain-controlled mechanisms of behaviour, respectively [15]. Here reference is made to the value of nominal strength terms, $V_{u,\mathrm{sh}}$, $V_{u,\mathrm{fl}}$, and $V_{u,\mathrm{sl}}$, which are considered to degrade with increasing imposed ductility, μ_Δ (i.e., even when flexural yielding is possible for $\mu_\Delta=1$, the relative hierarchy of the strength terms may be reversed for higher μ_Δ values, since the strength terms decay at different rates.) To evaluate these terms, what is needed is an immediate tool by which to transform forces and strains from the local level, where some type of material failure has been detected, to the global level, where prioritizing of strength components and addition of scaled deformation capacity contributions is needed. The necessary transformations are described in the following sections.

34.3 Local to Global Transformation of Stress Resultants

Capacity prioritizing in order to identify the weakest link of member behaviour is done on the basis of member shear forces. Thus, although any possible form of failure refers to exhaustion of some material strength or deformation capacity, it

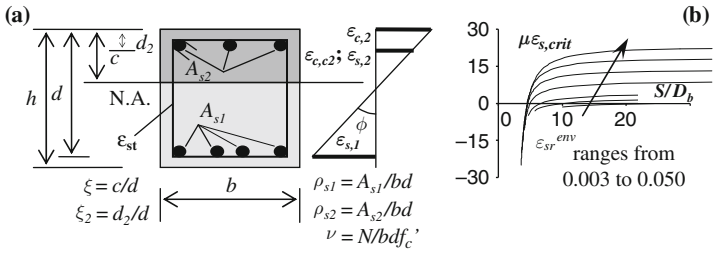

Fig. 34.3 (**a**) Definition of terms, (**b**) critical compr. strain ductility at bar buckling

is necessary that occurrence of this event be reflected in the global scale by the acting member shear force, V. With reference to Fig. 34.3a, possible material failure problems that would limit the strength of a column are:

(a) Cover delamination (i.e., max compr. strain $\varepsilon_{c,2}$ in the cover $\geq$ 0.0035–0.005).
(b) Confined concrete compressive strain at the extreme fiber of the confined zone, $\varepsilon_{c,c2}$, exceeds the strain capacity of the confined core, $\varepsilon_{c,\mathrm{cu}}$.
(c) Loss of concrete contribution to lap splice strength owing to longitudinal cover cracking due to load reversals (i.e., when $\varepsilon_{c,c2} > 0.002$).
(d) Bar strain $\varepsilon_{s,1}$ exceeds the strain development capacity of the reinforcement: $\varepsilon_{s,1} \geq \min\{\varepsilon_{s,1,\max}^{\text{anc - spl}};\ \varepsilon_{s,u}\}$ ($\varepsilon_{s,1,\max}^{\text{anc - spl}}$ is the tensile strain that may be sustained by the lap splice or anchorage at the critical section; $\varepsilon_{s,u}$ is the bar fracture strain.)
(e) Exhaustion of the compression strain capacity of longitudinal compression reinforcement (onset of bar buckling): $\varepsilon_{s,2} > \varepsilon_{s,\mathrm{crit}}$.
(f) Occurrence of web diagonal tension cracking: $V \geq V_{\mathrm{Rd1}}$ in [3] *or* V_c in [5,4].
(g) Onset of stirrup yielding, $\varepsilon_{\mathrm{st}} = \varepsilon_{\mathrm{st},y}$ (with regards to the nominal shear strength, V_{Rd3} in [3] or V_n in [5,4]).
(h) Occurrence of large postyielding strains in the stirrups (along the descending branch of the member response curve – associated with the degraded shear strength of the member, $V_{\mathrm{fl}}=V_{u,\mathrm{sh}}$, Eq. (34.3)): $\varepsilon_{\mathrm{st}} > \varepsilon_{\mathrm{st},y}$.

Equilibrium is used to convert from the material scale to the stress resultant of the cantilever of Fig. 34.1a (Eq. (34.2)). Normal strains over the cross section are assumed to follow a plane sections profile (Fig. 34.3a); for states of stress past flexural yielding, the normalized neutral axis depth, $\xi = c/d$, is assumed to remain approximately constant (its value may be obtained by interpolation using the gravity axial load, N_{g}, as a reference, average value [8]). Thus, for criteria (a) – (e) above, which refer to the occurrence of a milestone event in some component of normal strain, the corresponding shear force of the cantilever is obtained from:

$$V = M/L_s = \left[f_{s,1}A_{s1}d\,(1 - 0.4\xi) + N_g\,(0.5\,h - 0.4\xi d)\right]/L_s \tag{34.2}$$

In the above, $f_{s,1}$ is the axial stress in the steel tension reinforcement, for the corresponding axial strain, $\varepsilon_{s,1}$ (Fig. 34.3a) obtained from the steel stress-strain diagram. ($\varepsilon_{s,1}$ is the tension bar strain associated with each of the milestone events listed in (a)–(e) above: for case (a), $\varepsilon_{s,1}=\varepsilon_{c,2}(1-\xi)/\xi$; for (b), $\varepsilon_{s,1}=\varepsilon_{c,c2}(1-\xi)/(\xi-\delta_2)$, where $\delta_2=d_2/d$; for (c) and (d), the critical average bond stress $f_{b,u}$, acting over the active development length $L^u_{b,\text{eff}}$, can develop a tension bar stress $f^{\text{anc-spl}}_{s,1,\max}= 4f_b(L^u_{b,\text{eff}}/D_b)\leq f_{s,u}$; for case (e) the critical buckling strain is obtained from pertinent interaction diagrams that relate the dependable strain ductility of compression reinforcement, $\mu\varepsilon_{c,\text{crit}}$ with the normalized spacing of stirrups, S/D_b [15, 16], as shown in Fig. 34.3b – thus, the associated bar strain in the tension reinforcement, $\varepsilon_{s,1}$, is obtained from, $\varepsilon_{s,1}=\mu\varepsilon_{s,\text{crit}}\ \varepsilon_{s,y}(1-\xi)/(\xi-\delta_2)$.)

For criteria (f)–(h) the stress resultant is given by the shear strength of the cantilever model. After diagonal tension cracking of the web, the shear strength, denoted by V_n in [5, 4] or as V_{Rd3} in [3] is obtained from a Mörsch type truss for (g) and (h). Shear strength degrades with increasing magnitude of imposed displacement ductility, μ_Δ, due to compression softening of the concrete struts (reduction in f'_c) and thereby of the shear strength of the equivalent truss. Expressions to model this effect have been derived from first principles with reference to deterioration of dowel action, aggregate interlock, bond and diagonal tension cracking in cracked reinforced concrete [6]. Codes model this process using a simple reduction coefficient $k(\mu_\Delta)$,according with [3, 5, 4]:

$$V_{u,\text{sh}} = k(\mu_\Delta)\cdot(V_c + V_w) \tag{34.3}$$

where $k(\mu_\Delta)<1$ for $\mu_\Delta>1$ in [3], or for $\mu_\Delta>2$ in [5, 4] (i.e., after flexural yielding), whereby the process of degradation leads to a residual strength equal to 60% of V_n at $\mu_\Delta=6$ in [4], or to 75% of V_n at $\mu_\Delta=5$ in [3].

Values obtained for the milestone events listed above limit the strength of the mechanisms of resistance in series (Fig. 34.1b), namely *Flexural* ($V_{u,\text{fl}}$), *Shear* ($V_{u,\text{sh}}$), *Anchorage/Lap Splice* ($V_{u,\text{sl}}$), or *Compression Bar Stability* ($V_{u,\text{buckl}}$). Therefore, for any drift level, the above terms are organized in a hierarchy. The term with the lower strength, V_{fail}, controls the mode of damage and failure of the member:

$$V_{\text{fail}} = \min\{V_{u,\text{fl}}, V_{u,\text{sh}}, V_{u,\text{sl}}, V_{u,\text{buckl}}\} \tag{34.4}$$

This value is then used to estimate the coefficient w_u in Eq. (34.1).

34.4 Strain – Displacement Transformations

Geometric relations are required to identify the magnitude of column drift or tip displacement of the model cantilever (*strain resultants*), for each of the milestone events listed in the preceding section. Deformation mechanisms participating to total drift are illustrated in Fig. 34.2: they represent flexural drift due to curvature

along the member (Fig. 34.2b), rigid body rotation due to reinforcement pullout from the support anchorage or lap splice (Fig. 34.2c), and shear distortion which results in lateral offset of the member (Fig. 34.2d). Special considerations are as follows:

34.4.1 Strain Resultants Due to Flexural Curvature

34.4.1.1 Before Yielding of the Longitudinal Reinforcement

Chord rotation is $\theta = \Delta/L_s = \phi L_s/3$. At yielding, $\theta_y = \phi_y L_s/3$.

34.4.1.2 After Yielding of the Longitudinal Reinforcement

Inelastic flexural curvature is assumed to occur over a length of "plastic hinge", ℓ_p, measured from the face of the critical section. Inelastic tip displacement Δ_u and chord rotation θ_u or the associated plastic components Δ_{pl} and θ_{pl} are approximated by:

$$\Delta_u = \theta_u \cdot L_s; \quad \theta_u = \theta_y + \theta_{\text{pl}}; \quad \theta_{\text{pl}} = (\phi_u - \phi_y) \cdot \ell_p \cdot \big(1 - 0.5(\ell_p/L_s)\big) \approx \phi_u \ell_p \quad (34.5)$$

Definition of a Plastic Hinge Length, ℓ_{p}

The plastic hinge length ℓ_p was meant to account for spread of yielding along the length of the member. A consistent simple representation is obtained from the linear moment diagram along the shear span, which, for approximately constant internal lever arm after yielding, may be expressed in terms of the strain hardening ratio of main steel as per [8]:

$$\ell_p = [(f_{s,\max} - f_{s,y})/f_{s,\max}] \cdot L_s + a_v = \beta \cdot L_s + a_v \quad (34.6)$$

where $f_{s,\max}$ is the peak stress attained by the bar at the critical section whereas a_v is the moment-shift due to shear ($\approx 0.9d$). As $f_{s,\max}$ increases approaching the fracture strength of tension reinforcement, so does the ℓ_p value; thus, there is no unique value for ℓ_p, but it increases with demand. Various interpretations are associated with practical expressions for ℓ_p. For example, to account for yield penetration, and for extensive yielding, various alternative expressions have been proposed:

$$\ell_p = \omega_1 \cdot L_s + \omega_2 \cdot D_b \cdot f_y + \omega_3 \cdot h \quad (34.7)$$

where $\omega_1 = 0.08$, $\omega_2 = 0.022$ and $\omega_3 = 0$ in [10, 11], whereas $\omega_1 = 0.1$, $\omega_2 = 0.24/\sqrt{f_c'}$ and $\omega_3 = 0.17$ in [3]. At least two issues contribute to the uncertainty about ℓ_p: The first is that the formal definition for ℓ_p given by Eq. (34.6) breaks down if the steel reinforcement is elasto-plastic (no hardening), leading to $\ell_p \to 0$, which contradicts the expectation that yield penetration will spread over the anchorage in the absence of hardening. Another is the physical significance of the D_b-dependent term: it is

often associated with yield-penetration inside the support (anchorage), whereas an equal effect on θ_{pl} is also owing to yield penetration over the member length beyond the section of yielding moment (a term equivalent to a_v in Eq. (34.6)). Note that the most recent versions of the relevant assessment standards (e.g. in [4] and the revised draft of [3]) completely bypass the notion of a plastic hinge length by providing direct expressions for estimation of θ_{pl} without need for integration of inelastic curvatures. To eliminate the spurious outcome of Eq. (34.6) in practical applications, when the reinforcement exhibits little or no strain hardening, ℓ_p should be taken at least equal to $0.5d$.

34.4.2 Strain Resultants Owing to Bar Pullout/Slip

34.4.2.1 Before Yielding of Longitudinal Reinforcement

With reference to Fig. 34.2c, partial bar pullout from the support before yielding of longitudinal reinforcement causes a lumped rotation θ_{sl} at the support. This, in turn, produces a tip translation. The lumped rotation $\theta_{y,\text{sl}}$ at the onset of yielding is associated with a linear attenuation of bar strains from the yield strain value $\varepsilon_{s,y}$ at the column support, to zero over the effective anchorage length, $L^y_{b,\text{eff}}$, which is the length required to develop the bar yield force assuming a constant bond stress distribution equal to $f_{b,y}$ ($f_{b,y}$ is the *nominal code value* for bond strength [3, 2]).

$$\theta_{y,sl} = \phi_y L^y_{b,\text{eff}}/2; L^y_{b,\text{eff}} = D_b f_y/4 f_{b,y}; f_{b,y} = \eta_1 \cdot f'_t; \eta_1 = \begin{cases} 2.25 & \text{ribbed bars} \\ 1.0 & \text{smooth bars} \end{cases} \tag{34.8}$$

34.4.2.2 After Yielding of Longitudinal Reinforcement

Integration of bar strains over the part of the anchorage length where bar strains exceed yielding ($\varepsilon_{s,1} > \varepsilon_{s,y}$, ℓ_r = length of yield penetration over the anchorage) give a first order approximation of the plastic component of drift, associated with bar inelasticity over the anchorage:

$$\theta_{p,\text{sl}} = 0.5(\varepsilon_{s,u} + \varepsilon_y) \cdot \ell_r/[(1 - \xi) \cdot d] \tag{34.9}$$

34.4.2.3 Length of Yield Penetration in the Anchorage

To estimate the value of ℓ_r in Eq. (34.9), bond stress is assumed negligible over ℓ_r, corresponding to almost constant (post-yielding) bar stresses. (Note that if the definition of Section 34.4.2.2 is used instead, along with a nonzero strain hardening slope for the bar, the length of yield penetration may be estimated, by assuming a bi-linear distribution of bar stresses over the anchorage length. The slope of this diagram is: $4f_b/D_b$, where f_b the piecewise value of bond strength – a degraded value for the part of the anchorage that is beyond yielding, and the initial value, $f_{b,y}$, for the elastic part of the anchorage. This assumption leads to an expression for

ℓ_r Eq. (34.10) which is analogous to that obtained for the plastic hinge length, i.e., Eq. (34.6):

$$\theta_{p,\mathrm{sl}} = (\phi_u - \phi_y)\cdot\ell_r; \quad \ell_r = \frac{f_{s,\max} - f_{s,y}}{f_{s,\max}}\cdot\frac{D_b}{4}\cdot\frac{f_{s,\max}}{f_{b,u}} = \frac{\beta\cdot f_{s,\max}}{f_{b,u}}\cdot\frac{D_b}{4} = \frac{\beta\cdot f_{s,\max}}{f_{b,u}}\cdot\frac{D_b}{4} \tag{34.10}$$

Again, this breaks down for elastoplastic reinforcement without hardening, i.e., when β=0). To obtain ℓ_r for the general case, note that yield penetration cannot grow indefinitely: pullout failure of the anchorage occurs once the residual anchorage length engaged, equal to L_b–ℓ_r, exhausts the effective anchorage length, $L^u_{b,\mathrm{eff}}$ (note that $L^u_{b,\mathrm{eff}}$=$D_b f_y/4f_{b,u}$, which is the minimum length required to support the bar yield force, whereas L_b is the available anchorage length).

34.4.2.4 Limiting Strain Development Capacity After Yielding

Yield penetration limits the strain development capacity of the bar to the value: $\varepsilon^{\text{anc - spl}}_{s,1,\max}$=$\varepsilon_y L_{\mathrm{anc}}/L_{\mathrm{eff},u}$. This result is a consequence of the continuity of strain requirement at the end of yield penetration. Thus, even if the available anchorage length, L_b, suffices to develop the yield force of the bar, the strain that may be sustained at the face of the anchorage is limited eventually by yield penetration: Inelastic anchorage failure will occur when the bar strain exceeds the above-set limit for $\varepsilon^{\text{anc - spl}}_{s,1,\max}$.

34.4.2.5 Bond Strength in Eq. (34.10)

Ultimate bond strength, $f_{b,u}$, mobilized along a bar anchorage or lap splice is associated with the bar-concrete interface friction which depends on the clamping action provided by the surrounding concrete cover and transverse stirrups against the possible plane of splitting [15]:

$$f_{b,u} = 1.4\cdot\left(\underbrace{\frac{p}{D_b}f'_t}_{\text{cover}} + \underbrace{\frac{A_{st}\cdot f_{st,y}}{D_b\, n_b\, S}}_{\text{stirrups}}\right); \quad f'_t = 0.5\sqrt{f'_c} \tag{34.11}$$

n_b is the number of bars restrained by the stirrup legs included in A_{st} (where A_{st} is the cross sectional area of stirrups crossing the splitting plane). The concrete term depends on the critical crack path, p, required for splitting failure: p=$2.5D_b$+$2D_{st}$+$2c_o$ for lap-splices or anchorages outside the end support of the member, where c_o is the concrete cover thickness [11]. If the anchorage occurs in well confined regions (e.g. inside a column) the value of p in (11) is taken =$4c_o$ to account for plastification of the surrounding concrete prior to its pullout failure. Note that in lap-splices or anchorages that occur within the member's span (i.e. outside the end support), the cover contribution to $f_{b,u}$ is set to zero when the normal

compressive strain in the cover has exceeded the value of 0.002 to account for cover separation from the bar surface due to longitudinal splitting in the compression zone (Section 34.3c); thus a significant loss of development capacity occurs in situations past the above limit.

34.4.3 Distortion Resultants

34.4.3.1 Elastic Distortion Term

Shear distortion is elastic prior to web cracking, obtained from the acting shear force to the member's shear stiffness ratio [3, 10]:

$$\theta_{y,\mathrm{sh}} = V \big/ [0.4 \cdot E_c \cdot 0.8 A_g] \tag{34.12}$$

34.4.3.2 Distortion in the Plastic Hinge Region

After web cracking, shear distortion is set equal to stirrup strain, $\varepsilon_{\mathrm{st}}$. From the Mörsch truss geometry it may be shown that $\gamma = \varepsilon_{\mathrm{st}} = (V - V_{c,\mathrm{cr}}) / [E_s \Sigma A_{\mathrm{st},i}]$, where the numerator in this calculation represents the total force carried by the stirrups crossing a diagonal crack, V_w (Eq. (34.3)) and the denominator represents the extensional stiffness of the stirrups. Here, $V_{c,\mathrm{cr}}$ is the total shear force carried by the cracked concrete web:

$$\text{For } \frac{N}{f_c' \cdot A_g} \geq (\rho_{s1} - \rho_{s2}) \cdot \frac{f_y}{f_c'} \Rightarrow V_{c,\mathrm{cr}} = 0.5\sqrt{f_c'} \cdot \left[\frac{d}{L_s} \cdot \sqrt{1 + \frac{N}{0.5\sqrt{f_c'} \cdot A_g}} \right] \cdot A_g \tag{34.13}$$

Otherwise, $V_{c,\mathrm{cr}} = 0$. Note that Eq. (34.13) has been derived from equilibrium of forces on the cross section: a concrete contribution is assumed to exist if there is a nonzero compressive force in the concrete (i.e. once the cracks have been closed). With particular reference to columns with distributed reinforcement on all sides of the cross section, it is necessary to establish the neutral axis location prior to estimating the effective tension and compression reinforcement ratios, ρ_{s1}, ρ_{s2}, to be used with Eq. (34.13).

Furthermore, according with the CBP model, the contribution of web reinforcement to shear strength, V_w, should be calculated from the sum of forces developed in all stirrup legs crossing the critical shear crack, while also considering the limited development capacity of inadequately anchored stirrups: $V_w = A_{\mathrm{st}} \cdot \sum_i f_{\mathrm{st},i} \neq A_{\mathrm{st}} \cdot f_{y,\mathrm{st}} \cdot (d - d_{s2}) \big/ S$. Thus, for old-type construction it is necessary that stirrups be accounted for discretely and not smeared through the *d/S* term, as it is essential that the least number of stirrups crossing a crack plane need be determined, rather than an average value. If it is possible to determine a shear crack path along the member that does not interrupt any stirrup legs at all, then the V_w term according to the CBP

definition is zero [6], whereas the Codes [3, 5, 4] would yield a nonzero value even for excessively large stirrup spacing, *S*.

34.4.3.3 Degradation of Shear Strength

This phenomenon occurs after web cracking, as the value of the stirrup strain, ε_{st}, increases: assuming for simplicity that $V_{u,sh}$ follows the pattern adopted by ASCE-41, the stirrup strain, ε_{st}, is evaluated from the stirrup force: $V_w=[V-k(\mu_\Delta)\cdot V_{c,cr}]/\, k(\mu_\Delta) \rightarrow \varepsilon_{st} = V_w/E_s A_{st}$. The principal tensile concrete strain, $\varepsilon_{c1} \approx \sqrt{2}\varepsilon_{st}/2$ occurs in directions orthogonal to the concrete struts of the Mörsch truss causing the so-called compression softening of the struts according with the Modified Compression Field Theory. The compression softening coefficient is: $\lambda=1/(0.8+0.27\varepsilon_{c1}/\varepsilon_{co})$; this is responsible for the degradation of nominal shear strength, expressed empirically through $k(\mu_\Delta)$ [6].

The Angle of Sliding

An unresolved issue in calculations is the angle of inclination of the critical shear crack: a variety of tests (Fig. 34.4) demonstrate that aspect ratio and axial load ratio both affect the V_c and V_w terms; whereas this effect is considered in all alternatives for the concrete contribution term V_c (Eq. (34.3)), it is generally neglected by the Code Models and the Mechanistic expressions for V_w, which is generally obtained from a 45° crack assumption, as illustrated by the most prominent expressions for shear strength, Eqs. (34.14), (34.15), and (34.16). The model for V_n in [11] is a stark exception to this rule. Other differences between Eq. (34.14) and the N.A. code

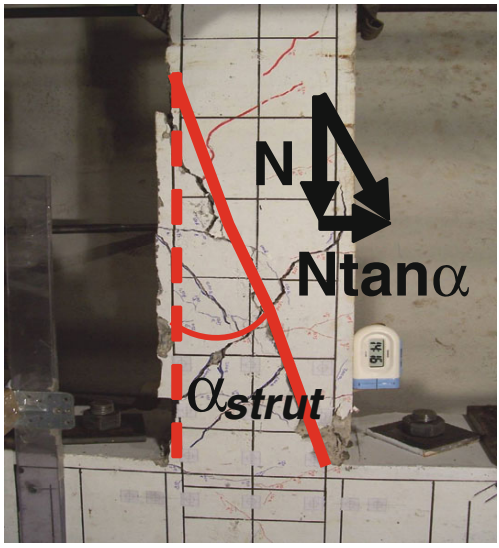

Fig. 34.4 Angle of sliding (inclination of critical shear crack) and contribution of axial load to shear resistance (=*N*tanα)

expression [5, 4] given by Eq. (34.15) are, (a) the standalone contribution to shear strength by the applied axial load, which is also adopted by [3] (Eq. (34.16)) and (b) that the strength degradation coefficient $k(\mu_\Delta)$ is not applied on the shear strength of the equivalent truss, a feature that is at odds with experimental evidence and basic fundamentals of Compression Field Theories for concrete. The uncertainty thus introduced in shear strength estimations can more than the account for the persistent dispersion in the available data on this variable.

$$V_n = V_c + V_N + V_w = k(\phi)\cdot\sqrt{f'_c}\cdot 0.8A_g + N\cdot\tan\alpha + \frac{A_{\mathrm{st}}f_{\mathrm{st},y}\,(d-d_2)}{S}\cdot\cot\alpha \quad \text{in [11]} \tag{34.14}$$

$$V_n = V_c + V_w = k(\mu_\Delta)\cdot\left[\frac{0.5\sqrt{f'_c}}{L_s/d}\sqrt{1+\frac{N}{0.5A_g\sqrt{f'_c}}}\right]\cdot 0.8A_g + k(\mu_\Delta)\cdot\frac{A_{\mathrm{st}}f_{\mathrm{st},y}d}{S} \text{ in [5, 4]} \tag{34.15}$$

$$V_{Rd3} = V_c + V_N + V_w = k(\mu_\Delta)(0.16\max(0.5; 100\rho_{tot})(1-0.16\min(5;\tfrac{L}{h})\cdot\sqrt{f'_c}\cdot 0.8A_g + \min\{N; 0.55A_e f'_c\}\tan\alpha + k(\mu_\Delta)A_{\mathrm{st}}f_{\mathrm{st},y}\cdot\left[\tfrac{d-d_2}{S}\right] \text{[in 5]} \tag{34.16}$$

34.4.4 Bar Buckling

It threatens members that do not fail prematurely, but undergo extensive flexural yielding. Due to load reversal the bar reaches instability conditions under a compression stress but with significant residual tensile strain [16]. The critical total strain ductility at buckling, $\mu\varepsilon_{s,\mathrm{crit}}$, is obtained from pertinent interaction diagrams that depend on the bar's unsupported length ratio S/D_b and the peak inelastic tension strain (envelope), attained by the reinforcement during previous displacement reversals, $\varepsilon_{sr}{}^{\mathrm{env}}$ [see Fig. 34.3(b) from [16].

34.5 The Correlation with Tests

To illustrate the effects on deformation capacity and on the controlling failure sequence imparted by important design parameters (such as the shear demand to supply ratio, sparse spacing and anchorage of stirrups, confinement in lap splice regions and pattern of imposed displacement history), an experimental study was conducted by the authors [14, 12]. The test program included 16 scaled column specimens with details representative of older practices ("non-conforming" as per [5, 4]), having a shear span $L_s = 0.9$ m, a 200 mm^2 cross section, reinforced with either eight or four longitudinal bars in order to effect a high and a low shear demand, respectively. Thus, either three or two main bars (D_b=12 mm) were arranged on each side of the cross section, respectively. Transverse reinforcement comprised smooth rectangular stirrups (D_{st}=6 mm), spaced as listed in Table 34.1.

Table 34.1 Specimen details. In all cases, clear cover = 20 mm, Long. Reinf.: D_b=12 mm, Transv. Reinf.: D_{st}=6 mm (smooth); Lines 6 and 7 list the peak shear force sustained, P_{max} (kN) and the corresp. drift capacity θ_u (%). Cases marked with * had: f_y=524 (MPa), $f_{st,y}$=271; all others had f_y=623 and $f_{st,y}$=384. Case 9b had 2 layers of stirrups at S=140 mm

Group I: Long. Reinf. = 8 bars											**Group :** L.R.= 4 bars				
1a*	1b*	2a*	2b*	3a*	3b*	4a	4aa*	4b*	5a*	5b*	7a	7b	8a	8b	9b
S=50 mm		S=70 mm (stirrup spacing in mm)							110 mm		70 mm		110 mm		140
No lap splice				L_{spl}=25D_b		L_{spl}=36D_b					No lap splice				
f'_c = 20.2 (MPa)						40.8 f'_c = 25.5 (MPa)					f'_c = 40.8 (MPa)				
52.8	54.1	50.2	51.1	33.0	32.4	58.1	46.0	40.8	52.6	52.4	37.8	36.7	37.1	37.3	38.9
4.4	4.5	2.1	3.7	2.25	2.0	6.3	1.9	1.6	2.25	6.15	7.25	13.2	6.05	6.9	13.3

Bars in 5 specimens were lap spliced at the base above the footing, over a length of either 25D_b or 36D_b (Table 34.1). Specimens were tested under a constant axial load $N \approx 0.1 f_c' A_g$, and lateral displacement reversals following two different displacement histories identified by index "a", "aa" or "b" in Table 34.1 [14, 12].

All specimens failed in a brittle mode. Deformation capacity and lateral strength (average value in the two directions) are listed in Table 34.1. The tests showed that flexural shear and anchorage strengths degraded at different rates with increasing displacement, confirming the basic thesis of the mechanical model regarding capacity prioritization as prerequisite in assessing deformation capacity.

The mechanistic principles outlined in this paper as well as in Code Models [3, 5, 4] were used to evaluate the strength terms (V_{flex}, $V_{u,sh}$, $V_{u,sl}$) and deformation capacities (θ_y, θ_u) of the test specimens using the actual material properties. Results are compared with the experimental values (both from tests "a" and "b" for otherwise identical specimens in each subgroup) in Fig. 34.5. Discrepancies are observed in the estimated strength of laps according with [4]; all models tend to overestimate rotation at yielding, but provide conservative estimates of rotation capacity.

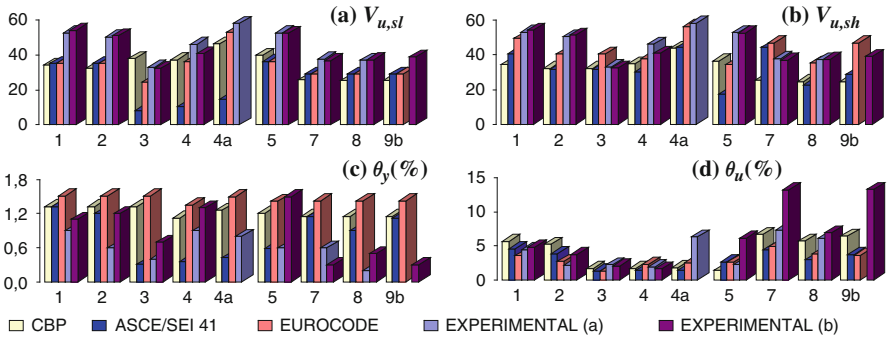

Fig. 34.5 Comparison between analytical and experimental results: $V_{u,sl}$, $V_{u,sh}$, θ_y, θ_u

Discrepancies are mostly inherited by the deviation in the values of estimated residual shear and lap strengths, which remain the least adequately understood variables from among the strength terms in the hierarchy of Eq. (34.4).

References

1. Berry M, Parrish M, Eberhard M (2004), PEER structural performance database – user's manual, PEER Center, University of California, Berkeley, CA
2. CEN (2003) EN 1992-1-1:2003 – Eurocode 2 -design of concrete structures. Part 1: general rules and rules for buildings". European Committee for Standardisation, Brussels
3. CEN (2005) EN 1998-3:2005 – Eurocode 8 Design of structures for earthquake resistance – part 3: assessment and retrofitting of buildings", European Committee for Standardisation, Brussels
4. Elwood K, Matamoros A, Wallace J, Lehman D, Heintz J, Mitchell A, Moore M, Valley M, Lowes L, Comartin C, Moehle J (2007) Update to ASCE/SEI 41 concrete provisions. Earthq Spectra 23(3):493–523
5. FEMA 356 (2000) Prestandard and commentary for the seismic rehabilitation of buildings. FEMA, Washington, DC
6. Martin-Perez B, and Pantazopoulou S (2001) Effect of bond, aggregate interlock and dowel action on shear-strength degradation of reinforced concrete. Eng Struct 23:214–227
7. Panagiotakos T, Fardis MN (2001) "Deformation of R.C. members at yielding and ultimate", ACI Struct J 98(2):135–148
8. Pantazopoulou SJ (2003) Chapter 4 in "Seismic assessment and retrofit of reinforced concrete buildings", fib Bulletin No. 24, fib, Lausanne, Switzerland
9. Park R, Paulay T (1975) Reinforced concrete structures. Wiley, New York, NY, p 769
10. Paulay T, Priestley MJN (1992) Seismic design of reinforced concrete and masonry buildings. Wiley, New York, NY, 767 pp
11. Priestley MJN, Seible F, Calvi M (1996) Seismic design and retrofit of bridges. Wiley, New York, NY
12. Syntzirma D, Thermou G, Pantazopoulou S, Halkitis G (2006) Experimental research of R.C. elements with substandard details, 1st European conference on earthquake engineering and seismology, Geneva, paper no: 819
13. Syntzirma DV, Pantazopoulou SJ (2002) Performance-based seismic evaluation of R.C. building members", 12th European conference on earthquake engineering, London, paper no:816
14. Syntzirma DV, Pantazopoulou SJ (2006) Assessment of deformability of R.C. members with substandard details. 2nd international fib congress, Naples, Italy, 5–8 June, paper no. 446
15. Syntzirma DV, Pantazopoulou SJ (2007) Deformation capacity of R.C. members with brittle details under cyclic loads. ACI Special Publ 236:1–22
16. Syntzirma DV, Pantazopoulou SJ, Aschheim M (2010) Load history effects on deformation capacity of flexural members limited by bar buckling. J Struct Eng ASCE 136:1–11